MULTI-SCALE ANALYSIS OF NOISE-SENSITIVITY NEAR A BIFURCATION

R. Kuske
University of British Columbia
#121-1984 Mathematics Road
Vancouver, BC V6T 1Z2
rachel@math.ubc.ca

Abstract We develop a multi-scale analysis for stochastic differential equations. Such models are particularly sensitive to noise when the system is near a critical point, such as a Hopf bifurcation, which marks a transition to oscillatory behavior. In particular, we are interested in the case when the combined effects of the noise and the bifurcation amplify oscillations which would decay in the deterministic system. The derivation of reduced equations for the envelope of the oscillations provides an efficient analysis of the dynamics by separating the influence of the noise from the intrinsic oscillations over long time scales.

Keywords: Stochastic, bifurcation, Duffing-van der Pol, multiple scales, amplitude equations

1. Introduction

In this paper we give an asymptotic analysis of the effect of noise near a Hopf bifurcation for the stochastic Duffing-van der Pol equation. In particular, we are interested in the case where the sensitivity to the noise is demonstrated through a resonance. In the presence of noise, oscillations are sustained in the subcritical region, where oscillations die out in the absence of noise, as shown in Figure 1. In the absence of external periodic forcing this phenomenon has been called autonomous stochastic resonance [1], where the noise excites the oscillations intrinsic to the deterministic dynamics. It has been observed in many systems with delays, including models of neurons, lasers, and a variety of oscillators with delayed feedback (see [2]-[6], and references therein). It has also been observed in systems without delays, where it has been studied in the context of stochastic bifurcations [7].

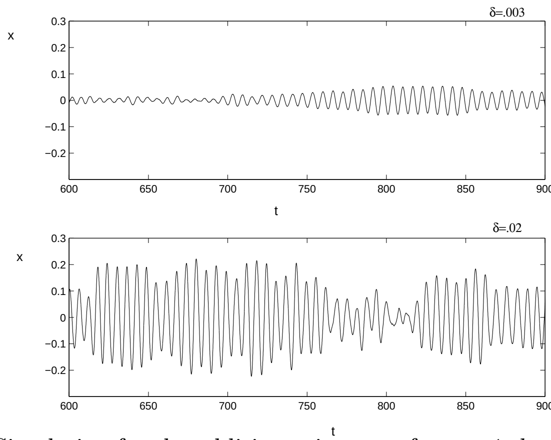

Figure 1. Simulation for the additive noise case, for $a = 1$, $b = 1$, $\beta = -\epsilon^2$, $\epsilon = .07$. In the top figure $\delta = .003$, and the bottom figure $\delta = .02$. Even though ϵ is the same for both, the bottom figure has larger amplitude oscillations.

In this paper we consider a canonical example of a system, the Duffing-van der Pol equation, which has been studied both in the context of deterministic and stochastic cases. We will consider both additive and multiplicative noise cases. Using multi-scale analysis, we derive envelope equations for the stochastic amplitude of the oscillations. We see that this approach leads to results similar to those in [8]-[11]. The multi-scale approach provides a new viewpoint of the dynamics in which the oscillations have the deterministic frequency associated with the Hopf bifurcation and are modulated by a slowly varying stochastic amplitude. It also has an attractive physical interpretation which is directly related to resonance with Fourier-type components.

2. Multi-scale analysis

We begin with the Duffing-van der Pol equation with additive noise, which we write as a system of stochastic differential equations.

$$dx = ydt \tag{1}$$

$$dy = \left[-\omega^2 x + \beta y - ax^3 - bx^2 y\right] dt + \delta dw. \tag{2}$$

For comparison, we also consider multiplicative noise, replacing (2 with

$$dy = \left[-\omega^2 x + \beta y - ax^3 - bx^2 y\right] dt + \delta x dw. \tag{3}$$

We are interested in the case where β is near zero, since $\beta = 0$ corresponds to a Hopf bifurcation in the absence of noise. That is, for $\beta < 0$ oscillations decay over time and for $\beta > 0$ there is a stable oscillatory behavior. We will explore the noise-sensitivity of the system for small values of β, restricting our analysis to $\delta \ll 1$ in order to understand where small noise can play a significant role in the dynamics. We will obtain relevant scalings related to this noise-sensitivity. In order to focus on these parameters, we set all other parameters to unity, $\omega = a = b = 1$.

It is well known that in the absence of noise ($\delta = 0$), one can give an asymptotic approximation to the solution when the parameters correspond to close proximity to the Hopf bifurcation. The method of multiple scales is useful for giving a description in which the natural mode of oscillation associated with the bifurcation appears explicitly in the approximation [12]. The form is

$$x \sim A(T)\cos\omega t + B(T)\sin\omega t, \quad T = \epsilon^2 t, \tag{4}$$

where ϵ^2 is the parameter measuring the proximity to the bifurcation. Here $A(T)$ and $B(T)$ are functions of a slow time T, which are treated as constants with respect to the fast oscillations with frequency ω on the t time scale. By deriving equations on the slow T scale for the amplitude, or envelope, described by $A(T)$ and $B(T)$, one gets an asymptotic approximation for the process near the Hopf bifurcation, that is, for $\epsilon^2 \ll 1$. In the remainder of this paper, we derive such envelope or amplitude equations in the stochastic case $\delta \neq 0$.

2.1 Additive noise: $\beta < 0$

We begin by considering the subcritical case with additive noise (2). In the absence of noise, oscillations decay exponentially in time. In the case of additive noise, the noise causes a resonance-type effect in exciting the natural modes of the system, even when the noise is small (See Figure 1). This is particularly evident when $|\beta| \ll 1$, that is, β takes values near the Hopf bifurcation point of the deterministic system.

We borrow techniques from the derivation of envelope equations via multi-scale analysis, used in studying the bifurcations of patterns near critical [12]-[13]. The analysis starts with the identification of a slow time scale $T = \epsilon^2 t$, which is related to the proximity of β to zero, $\beta = \epsilon^2\beta_2$, for $\beta_2 = O(1)$ with respect to ϵ. Note that $\beta_2 < 0$ in the subcritical case. Then we look for an asymptotic approximation to the solution in the form of a slowly varying amplitude, or envelope, and for the critical mode corresponding to the Hopf bifurcation. A standard linear analysis of the deterministic system shows that this critical mode has frequency ω. Therefore, we expect approximations of the form

$$\hat{x}(t) \quad = \quad \epsilon A(T)\cos\omega t + \epsilon B(T)\sin\omega t. \tag{5}$$

Here we have assumed that $A(T)$ and $B(T)$ are slowly varying functions of time, which is appropriate when $\epsilon \ll 1$ and $\delta \ll 1$. Below we

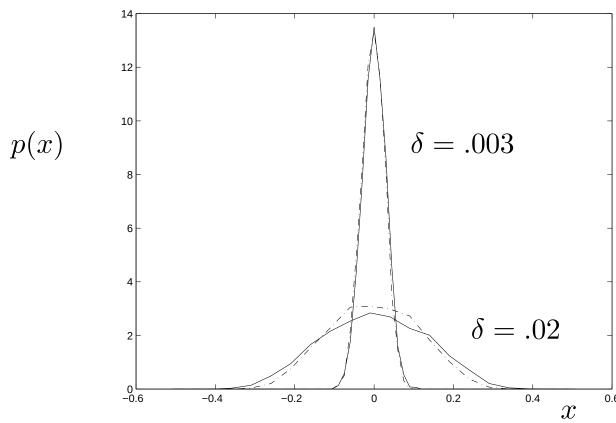

Figure 2. The probability density function $p(x)$ and $p(\hat{x})$, obtained from 5000 numerical simulations of the full system (2) (dash-dotted lines) and the multi-scale approximation (solid line) for $a = 1$, $b = 1$, $\beta = -\epsilon^2$, $\epsilon = .07$ for large t. Here t is chosen sufficiently large in order to approximate the invariant density for additive noise. The two sets of curves correspond to two different noise levels, $\delta = .003$ and $\delta = .02$, giving more and less concentrated densities, respectively.

also determine the relationship between δ and ϵ for the validity of the asymptotic approximation.

We derive equations for $A(T)$ and $B(T)$ of the form

$$dA = \psi_A dT + \sigma_A d\xi_1(T), \quad dB = \psi_B dT + \sigma_B d\xi_2(T), \tag{6}$$

with $\xi_1(T)$ and $\xi_2(T)$ as independent standard Brownian motions.

In order to get the drift coefficients ψ_A, ψ_B and the diffusion coefficients σ_A, σ_B, we use two identities expressing $d\hat{x}$ and $d\hat{y}$ in terms of A and B. In the Appendix we use multi-scale analysis to obtain the leading order approximation for the coefficients,

$$\psi_A = \frac{1}{2}\beta_2 A + \frac{3}{8}aB(A^2+B^2) - \frac{1}{8}bA(A^2+B^2), \tag{7}$$

$$\psi_B = \frac{1}{2}\beta_2 B - \frac{3}{8}aA(A^2+B^2) - \frac{1}{8}bB(A^2+B^2),$$

$$\sigma_A = -\frac{\delta}{2\epsilon^2}, \quad \sigma_B = \frac{\delta}{2\epsilon^2}. \tag{8}$$

Note that ψ_A and ψ_B are identical to the result of the multiscale analysis in the deterministic case.

From (8) we can conclude that the multiscale analysis is valid when the magnitude of the noise is $\delta = O(\epsilon^2)$ or smaller. For $\delta \gg \epsilon^2$, we see that the noise dominates the dynamics of the envelope. Then it is inappropriate to use the multi-scale approximation in which the envelope is a slowly varying stochastic process. This scaling relationship $\delta \sim \epsilon^2$

is not unexpected, since it appears in other analyses of the non-trivial behavior of this system near the Hopf bifurcation [8]-[11].

Using (6)-(8) we numerically simulate the solution for $A(T)$ and $B(T)$ for $\delta = O(\epsilon^2)$, and thus obtain the approximation $\hat{x}$ for $x(t)$. Since this approximation holds in an averaged or weak sense, we compare the results by comparing simulations which approximation the probability density, as shown in Figure 2. Note that the simulation of the multi-scale approximation is approximately $O(1/\epsilon^2)$ faster than the simulation of the original model (2), since the approximation (5) requires the simulation of (6) on the T time scale rather than the t time scale.

2.2 Multiplicative noise: $\beta < 0$

The procedure for approximating x in (3) for this case is similar to that described in the previous section. We again use the form (5) for $\hat{x}$.

As in Baxendale [8]-[9], we assume the form of equations for A and B

$$\begin{pmatrix} dA \\ dB \end{pmatrix} = \begin{pmatrix} \psi_A \\ \psi_B \end{pmatrix} dT + \sum_{j=1}^{3} \Sigma_j \begin{pmatrix} A \\ B \end{pmatrix} d\mathcal{W}_j(T). \tag{9}$$

Here the drift coefficients ψ_A and ψ_B are the same as in the additive noise case, but the noise is in terms of three independent Brownian motions $\mathcal{W}_j$. In [9] it is shown that the averaged equations for the stochastic van der Pol-Duffing equation have this form, in particular for describing the two-point motion and the associated Lyapunov exponent. The constant matrices Σ_j follow from a consistency comparison of the infinitesimal generators for the original and averaged processes.

$$\Sigma_0 = \frac{c_0}{2}\begin{bmatrix} 0 & 1 \\ -1 & 0 \end{bmatrix} \quad \Sigma_1 = \frac{c_1}{2\sqrt{2}}\begin{bmatrix} 1 & 0 \\ 0 & -1 \end{bmatrix} \quad \Sigma_2 = \frac{c_2}{2\sqrt{2}}\begin{bmatrix} 0 & 1 \\ 1 & 0 \end{bmatrix}. \tag{10}$$

Here c_j depends on the small parameters δ and ϵ.

Our multi-scale analysis gives the same form for the noise terms in the stochastic amplitude equations for the delay equation with multiplicative noise. This can be seen by writing the noise as a type of Fourier series representation,

$$\delta Sx(t)dw = \delta\mathcal{M}_0\overline{x}dw_0 + \delta\mathcal{M}_1\overline{x}\cos 2\omega t dw_1 + \delta\mathcal{M}_2\overline{x}\sin 2\omega t dw_2. \tag{11}$$

where

$$S = \begin{bmatrix} 0 & 0 \\ 1 & 0 \end{bmatrix}, \quad \overline{x} = (x\ y)^T, \quad \mathcal{M}_j = \begin{bmatrix} m_{j1} & m_{j2} \\ m_{j3} & m_{j4} \end{bmatrix}, \tag{12}$$

w_j are independent Brownian motions, and $\mathcal{M}_j$ are constant matrices that must be determined. Note that we could include other modes in

(11), such as $\mathcal{M}\overline{x}\sin k\omega t$ for $k > 2$. However, under the multi-scale projection onto $\cos\omega t$ and $\sin\omega t$ as shown in the Appendix (A.10), these terms do not contribute to the stochastic amplitude equations. In addition, there are certain restrictions on the coefficients m_{jk}, as discussed below. This forces us to express the term $Sx(t)dw$ in more than one term of such a Fourier representation. Here we retain all terms which would possibly contribute to the leading order behavior of the envelope, due to a resonance with the dominant mode $\cos\omega t,\ \sin\omega t$.

As in the case of additive noise, we write $w_j(t) = \mathcal{W}_j(T)/\epsilon$ and use the multi-scale projection (A.10) onto $\cos\omega t$ and $\sin\omega t$, treating $\mathcal{W}_j(T)$ as independent of t. This gives m_{jk} in terms of the entries for Σ_j.

$$m_{01} + m_{04} = 0 \quad m_{12} - m_{13} = c_0\frac{\epsilon}{\delta} \tag{13}$$

$$m_{j1} - m_{j4} = \frac{c_j\epsilon}{\delta\sqrt{2}}, \quad m_{j2} + m_{j3} = 0, \quad j = 1, 2 \tag{14}$$

Note that there is not a unique solution to this system, so we have some freedom in choosing the matrices $\mathcal{M}_j$. For example, we can take $m_{03} = -1$, $m_{14} = m_{24} = -1/\sqrt{2}$, and all other $m_{jk} = 0$, so that $c_0 = c_1 = c_2 = \delta/\epsilon$ agrees with Σ_j [9].

For the subcritical case with multiplicative noise, the deterministic decay plays a role in both the deterministic and stochastic aspects of the dynamics, and thus the noise does not dominate the behavior as in the case of additive noise. In Figure 3 we compare the time dependent probability density function for the original and multi-scale systems, observing how the shape of the density changes over time. In [8]-[11] the scaling $\delta = \epsilon$ is also used to obtain averaged equations of the same form as the envelope equations for A and B, and they show that an explicit expression for the probability density can be obtained for the averaged system. In [11], only two terms are used to represent the noise in the averaged system.

3. Supercritical case: $\boldsymbol{\beta > 0}$

For the supercritical case, we take $\beta = \epsilon^2\beta_2$ with $\beta_2 > 0$. In the absence of noise, oscillations are stable, which are approximated by

$$x \sim \epsilon\rho\cos((1+\epsilon^2\omega_2)t), \quad \rho^2 = 4\frac{\beta_2}{b}, \quad \omega_2 = \frac{3}{8}a\rho^2. \tag{15}$$

Then the multiscale approximation has the form

$$\hat{x} = \epsilon(\rho + A(T))\cos((1+\epsilon^2\omega_2)t) + \epsilon B(T)\sin((1+\epsilon^2\omega_2)t). \tag{16}$$

We restrict our attention to the case of additive noise, noting that the multiplicative noise can be treated in a similar way.

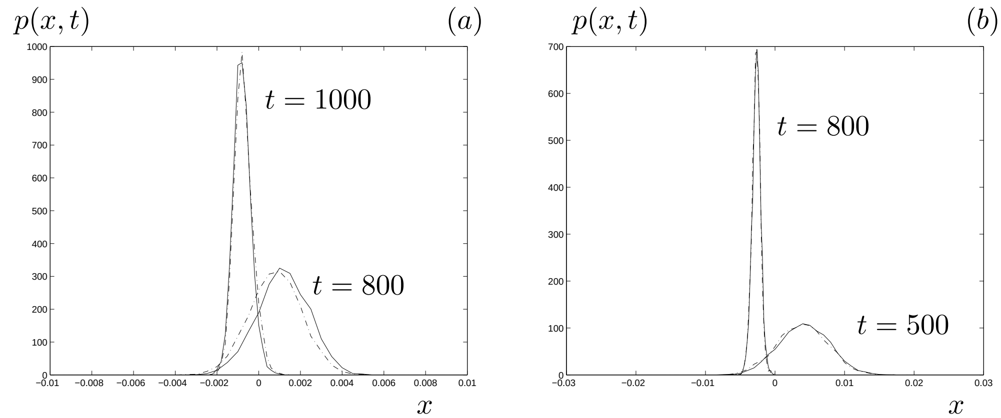

Figure 3. The probability density function $p(x,t)$ and $p(\hat{x},t)$, obtained from the simulation of the full system (3) (dash-dotted lines) and the multi-scale approximation $\hat{x}$ (solid line) for $a = 1$, $b = 1$, $\beta = -\epsilon^2$, $\epsilon = .1$, and $\delta = .02$. In (a) the results are graphed for two different times, $t = 800$ and $t = 1000$ and initial condition, $x(0) = .5, y(0) = 0$. In (b) we graph the density for two different times $t = 500$ and $t = 800$ and initial condition $x(0) = .25$, $y(0) = 0$.

Using the same multi-scale method to obtain the multi-scale approximation as in Section 2.1, we find that $A(T)$ and $B(T)$ in (16) follow the stochastic system of the form (6). In this case, the coefficients are

$$\begin{aligned}\psi_A &= -\beta_2 A - \omega_2 B + \frac{3}{8}a\rho^2 B + \frac{3}{4}a\rho AB - \frac{1}{8}b\rho\left(\frac{3}{4}A^2 + B^2\right) + \\ &\quad \frac{3}{8}aB(A^2+B^2) - \frac{1}{8}bA(A^2+B^2), \\ \psi_B &= \omega_2 A - \frac{9}{8}a\rho^2 A - \frac{1}{4}b\rho AB - \frac{3}{8}a\rho\left(\frac{3}{4}A^2 + B^2\right) - \\ &\quad \frac{3}{8}aA(A^2+B^2) - \frac{1}{8}bB(A^2+B^2). \end{aligned} \tag{17}$$

and σ_A and σ_B are given by (8). Once again ψ_A and ψ_B are identical to the result of the multiscale analysis in the deterministic case. In Figure 4 we compare the probability densities obtained from simulation of the original variable x, and the multi-scale approximation using (16) for $\hat{x}$ with (6), (8), and (17).

4. Summary

We apply a multiscale analysis to analyze the effect of noise on the canonical model of the stochastic Duffing-van der Pol equation. This model is particularly sensitive to noise when the delay is near a critical value, corresponding to a Hopf bifurcation. In the subcritical case, os-

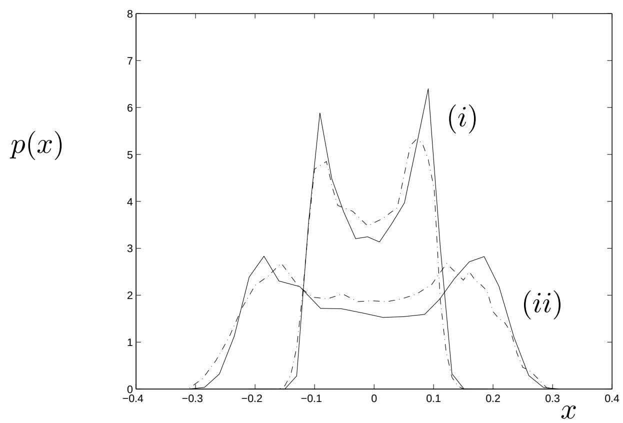

Figure 4. The probability density function $p(x)$ and $p(\hat{x})$, obtained from the numerical simulations (24,000 realizations) of the full system (dash-dotted lines) and the multi-scale approximation (16) (solid line) for $a = 1$, $b = 1$, $\beta = \epsilon^2$, for two cases: (i) $\epsilon = .05$ and $\delta = .002$ and (ii) $\epsilon = .1$ and $\delta = .01$. Here t is chosen sufficiently large so that it is anticipated that $p(x)$ is the invariant density for the case when the noise is additive. Note that a very large number of simulations is needed to completely resolve the density.

cillations which would decay in the absence of noise are amplified by the interaction of the noise and the bifurcation. We derive stochastic equations for the slow evolution of the envelope of these oscillations at the Hopf frequency. The analysis leads to a description which separates the deterministic and stochastic elements of the dynamics. Advantages of this approximation include efficiency of simulations over large times and relatively simple dynamics described by the envelope equations. The analysis also leads to a natural scaling between the magnitude of the noise δ and the proximity to the bifurcation ϵ^2. Note it is not necessary to assume this scaling relationship at the beginning of the analysis; it appears naturally as a result of the analysis, from which it is clear that the analysis is valid for $\delta = O(\epsilon^2)$ for additive noise, and $\delta = O(\epsilon)$ for multiplicative noise.

The method has also been applied to stochastic systems with delay: a linear system and the logistic model, both with delay and additive small noise [14], and a canonical model with delayed negative feedback [15]. For the linear system the approximation is compared with a result obtained from the Fourier analysis. For the logistic model both the sub- and super-critical cases are considered; that is, the analysis is applied for delays above and below the critical delay. The method is particularly useful for systems with delays since it avoids complications due to the memory in the system, which can make other analyses impractical.

The phenomenon demonstrated here occurs in many applications with similar features, including neuronal models, optics, and information systems [2]-[6]. The analysis exploits the interaction of the noise with the Hopf bifurcation, features which are common to these other models. Thus the analysis can be applied to a wide variety of stochastic models, in order to understand the effects of noise near a bifurcation.

Acknowledgments

The author wishes to thank Prof. Salah Mohammed for encouragements and useful discussions for this work.

Appendix: Details of the multi-scale analysis

We start with (2) and the ansatz for the multi-scale approximation (5)-(6). We also need the expression for $\hat{y}(t)$ which is

$$\hat{y}(t) = -\epsilon\omega \left[A(T)\sin\omega t - B(T)\cos\omega t\right]. \tag{A.1}$$

First, from Ito's formula, we have

$$\begin{aligned} d\hat{x} &= \frac{\partial\hat{x}}{\partial t}dt + \frac{d\hat{x}}{dA}dA + \frac{d\hat{x}}{dB}dB && \text{(A.2)} \\ &= \hat{y}dt + \epsilon\cos\omega t(\psi_A dT + \sigma_A d\xi_1) + \epsilon\sin\omega t(\psi_B dT + \sigma_B d\xi_2) \\ d\hat{y} &= \frac{\partial\hat{y}}{\partial t}dt + \frac{d\hat{y}}{dA}dA + \frac{d\hat{y}}{dB}dB && \text{(A.3)} \\ &= \left[-\omega^2\hat{x}\right]dt - \epsilon\omega\sin\omega t(\psi_A dT + \sigma_A d\xi_1) + \epsilon\omega\cos\omega t(\psi_B dT + \sigma_B d\xi_2). \end{aligned}$$

Here we have left out terms such as $\frac{d^2\hat{x}}{dA^2}$ and $\frac{d^2\hat{y}}{dB^2}$, since these quantities vanish, according to (5) and (A.1). The second set of expressions for $d\hat{x}$, $d\hat{y}$ comes from substituting (5) and (A.1) into (2),

$$\begin{aligned} d\hat{x} &= \left[-\epsilon(A(T)\sin\omega t + B(T)\cos\omega t)\right]dt && \text{(A.4)} \\ d\hat{y} &= \epsilon\left[-\omega^2(A(T)\cos\omega t + B(T)\sin\omega t) - \epsilon^2\omega\beta_2(A(T)\sin\omega t - B(T)\cos\omega t)\right. \\ &\quad -a\epsilon^2(A(T)\cos\omega t + B(T)\sin\omega t)^3 && \text{(A.5)} \\ &\quad \left.-b\omega\epsilon^2(A(T)\cos\omega t + B(T)\sin\omega t)^2(-A(T)\sin\omega t + B(T)\cos\omega t)\right]dt + \delta dw. \end{aligned}$$

Now we set (A.4) and (A.5) equal to (A.2) and (A.3), and collect coefficients of like powers of ϵ, noting the $dT = \epsilon^2 dt$. We find that the $O(\epsilon)$ terms cancel. Then the next terms are $O(\epsilon^3)$, and for convenience we write them in terms of the slow time T.

$$(\cos\omega t\,\psi_A + \sin\omega t\,\psi_B)dT + \cos\omega t\,\sigma_A\,d\xi_1 + \sin\omega t\,\sigma_B\,d\xi_2 = 0 \tag{A.6}$$

$$\begin{aligned} \epsilon(-\sin\omega t\,\psi_A + \cos\omega t\,\psi_B)dT + \epsilon(-\sin\omega t\,\sigma_A\,d\xi_1 + \cos\omega t\,\sigma_B\,d\xi_2) &= \\ \epsilon[-\beta_2(A(T)\sin\omega t - B(T)\cos\omega t) - a(A(T)\cos\omega t + B(T)\sin\omega t)^3 & \\ -b(A(T)\cos\omega t + B(T)\sin\omega t)^2(-A(T)\sin\omega t + B(T)\cos\omega t)]dT + \delta dw. & \qquad \text{(A.7)} \end{aligned}$$

Here we have used $\omega = 1$ in the coefficients. Then we equate the drift and diffusion terms. For the diffusion terms we have

$$\begin{aligned} \cos\omega t\,\sigma_A\,d\xi_1 + \sin\omega t\,\sigma_B\,d\xi_2 &= 0 && \text{(A.8)} \\ \epsilon(-\sin\omega t\,\sigma_A\,d\xi_1 + \cos\omega t\,\sigma_B\,d\xi_2) &= \delta dw && \text{(A.9)} \\ &= \frac{\delta}{\epsilon}\left[\cos\omega t\,dw_1(T) + \sin\omega t\,dw_2(T)\right] \end{aligned}$$

Here we have used well-known identities, first to express dw in terms of $\sin\omega t$, $\cos\omega t$ and two independent Brownian motions w_2 and w_1, and second to write $w_2(t)$ and $w_1(t)$ as functions of the slow time T.

At this stage we employ the multi-scale assumption, that is, that the fast time scale t and the slow time scale T are independent. This is a useful approximation when $\epsilon \ll 1$. In order to obtain σ_A and σ_B, we eliminate the fast oscillations in t, integrating over one period $2\pi/\omega$, using the orthogonality of $\sin\omega t$ and $\cos\omega t$, and treating t and T as independent. For example,

$$\int_0^{2\pi/\omega} [\epsilon\cos\omega t \cdot (A.8) - \epsilon\sin\omega t \cdot (A.9)]\, dt \quad \Rightarrow \sigma_A = -\frac{\delta}{2\epsilon^2}. \qquad \text{(A.10)}$$

Similarly, $\sigma_B = \frac{\delta}{2\epsilon^2}$.

We use the same method to solve for the drift coefficients, substituting the drift terms from (A.6) and (A.7) for (A.8) and (A.9), respectively, into (A.10). Again treating functions of T as independent from t yields (7).

References

[1] H. Gang, T. Ditzinger, C. Z. Ning, and H. Haken, *Phys. Rev. Lett.* **71** 807 (1993).

[2] J. Garcia-Ojalvo and R. Roy, "Noise amplification in a stochastic Ikeda model", *Phys. Lett. A* **224** (1996), 51-56.

[3] S. Kim, Seon Hee Park, and H.-B. Pyo, "Stochastic resonance in coupled oscillator systems with time delay", *Phys. Rev. Lett.* **82** (1999) 1620-1623.

[4] J. L. Cabrera, J. Gorronogoitia, and F. J. de la Rubia, "Noise-correlation-time-mediated localization in random nonlinear dynamical systems", *Phys. Rev. Lett.* **82** (1999), 2816-2819.

[5] T. Ohira and Y. Sato, "Resonance with Noise and Delay", *Phys. Rev. Lett.* **82** (1999) 2811-2815.

[6] A. Beuter, J. Belair, and C. Labrie, "Feedback and delays in neurological diseases: a modeling study using dynamical systems", *Bull. Math. Bio.* **55** (1993) 525-541.

[7] *Stochastic dynamics*, H. Crauel and M. Gundlach, eds. Springer-Verlag, New York, (1999).

[8] P. Baxendale,"Lyapunov exponents and stability for the stochastic Duffing-van der Pol oscillator", this proceedings.

[9] P. Baxendale,"Stochastic averaging and asymptotic behavior of the stochastic Duffing-van der Pol equation, in review.

[10] N. Sri Namachchivaya, R. Sowers and L. Vedula, "Nonstandard Reduction of Noisy Duffing-van der Pol Equation", *J Dyn. Sys.* **16** (2001), 223-245.

[11] L. Arnold, N. Sri Namachchivaya and K. Schenk-Hoppe, Toward an understanding of the stochastic Hopf bifurcation: a case study. *Int. J. Bif. Chaos* **6** (1996), 1947-1975.

[12] J. Kevorkian And J. D. Cole, *Multiple Scale and Singular Perturbation Methods*, Springer-Verlag, New York, 1996.

[13] P. Manneville, *Dissipative Structures and Weak Turbulence*, (1990), Academic Press, San Diego (1990).

[14] R. Kuske and M. Malgorzata, "Multi-scale analysis of stochastic delay differential equations", preprint.

[15] R. Kuske, "Asymptotic analysis of noise-amplified oscillations for subcritical delays", *Differential Equations and Dynamical Systems*, to appear.